

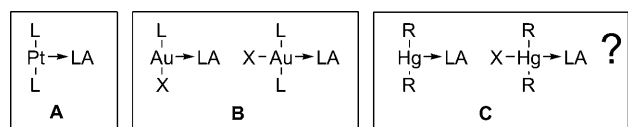
Metal–Metal Interactions

A Mercury → Antimony Interaction**

Tzu-Pin Lin, Casey R. Wade, Lisa M. Pérez, and François P. Gabbaï*

In the periodic table, mercury is classified as a post-transition metal element because it possesses a filled d shell in most of its compounds. In the past few decades, efforts to challenge this classification have been recurrent,^[1] leading, in 2007, to the observation of the d⁸ mercury complex HgF₄.^[2] This complex, the thermodynamic stability of which has been computationally established,^[3] was identified on the basis of a single IR band in the reaction of Hg with F₂ under photolytic conditions in a neon matrix at 4 K.^[4]

Unlike mercury, late transition metals, such as gold and platinum, form numerous complexes in which the metal involves its d electrons in bonding. Prototypical examples of such complexes include the d⁸ complexes AuCl₄[−] and PtCl₄^{2−}. More recently, it has been shown that these late transition metals can engage two of their d electrons in the formation of a dative bond with a Lewis acid to afford complexes of type **A**^[5] and **B**,^[6] among others.^[7] Although the electrons involved

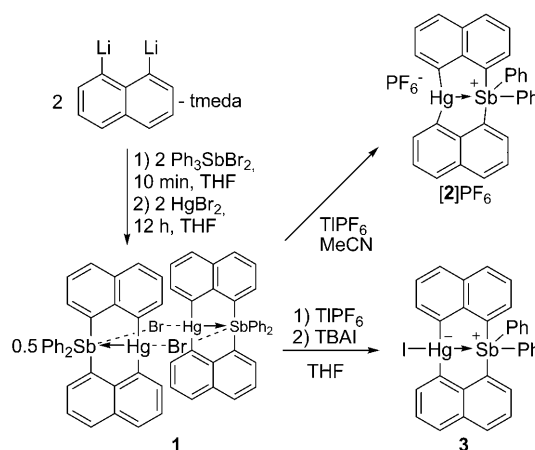


LA = Lewis acid, L = neutral ligand, X = halogen, R = aryl group

in the dative bond remain polarized toward the metal,^[6a,b] the ability of gold and platinum to form such interactions by donation of their d electrons is another signature of their transition metal identity. Stimulated by the notion that mercury might behave as a transition metal,^[2] we questioned whether complexes of type **C** could be observed.

To address this question, we sought a compound featuring a divalent mercury center held in close proximity to a highly Lewis acidic center. These considerations led us to select the 1,8-naphthalenediyl dinucleating ligand with a narrow bite angle that would promote a putative Hg→Lewis acid

interaction.^[8] The choice of the Lewis acid was dictated by a series of earlier studies that have shown that antimony(V) species are among the most potent Lewis acids.^[9] Reaction of 1,8-dilithionaphthalene^[10] with Ph₃SbBr₂ in THF followed by addition of HgBr₂ afforded **1** as a yellow solid in 54% yield (Scheme 1). This compound could be converted into the



Scheme 1. Synthesis of the mercury–antimony complexes. (TBAI = tetra-*n*-butylammonium iodide, tmeda = tetramethylethylenediamine.)

corresponding hexafluorophosphate salt **2-PF₆** by abstraction of the bromide anion with TIPF₆. Alternatively, reaction of **1** with TIPF₆ and subsequently TBAI (tetra-*n*-butylammonium iodide) afforded the iodide complex **3**. These compounds have been fully characterized. The ¹⁹⁹Hg NMR chemical shifts of complexes **1** (−68.2 ppm, [D₆]DMSO), **2-PF₆** (−271.9 ppm, [D₆]DMSO), and **3** (−71.8 ppm, [D₆]DMSO) exhibit a considerable downfield shift compared to that of Ph₂Hg (−808.5 ppm, [D₆]DMSO).^[11] This observed downfield shift is noteworthy and may reflect an increase in the coordination number of the mercury atom caused by coordination of solvent molecules, or a halide ligand in the case of **1** and **3**.^[12]

An examination of the crystal structure of [**2**]⁺ (Figure 1 a) indicates the presence of a dinuclear core with a short transannular mercury–antimony separation of 3.0601(7) Å.^[13] This separation, which lies between the sum of the metallic (3.17 Å) and covalent radii (2.71 Å) of the two elements, indicates that these two atoms are within bonding distance.^[14] Further inspection of the coordination environment of the mercury atom suggests a T-shape geometry, as indicated by the C1–Hg–Sb, C11–Hg–Sb, and C1–Hg–C11 angles of 87.1(2), 86.3(2), and 170.6(3)°, respectively. The secondary coordination sphere of the mercury atom also involves two hexafluorophosphate fluorine atoms that form weak contacts of 3.114(5) and 2.823(5) Å. The Hg–Sb–C21 angle of 174.2(2)°

[*] T.-P. Lin, C. R. Wade, Dr. F. P. Gabbaï
Department of Chemistry, Texas A&M University
College Station, TX 77843 (USA)
E-mail: francois@tamu.edu
Homepage: <http://www.chem.tamu.edu/rgroup/gabbaï>
Dr. L. M. Pérez
Laboratory for Molecular Simulation, Texas A&M University
College Station, TX 77843 (USA)

[**] Support by the National Science Foundation (CHE-0646916 and CHE-0952912), the Welch Foundation (A-1423), Texas A&M University (Davidson Professorship), and the Laboratory for Molecular Simulation at Texas A&M University (software and computation resources) is gratefully acknowledged.

Supporting information for this article is available on the WWW under <http://dx.doi.org/10.1002/anie.201002995>.

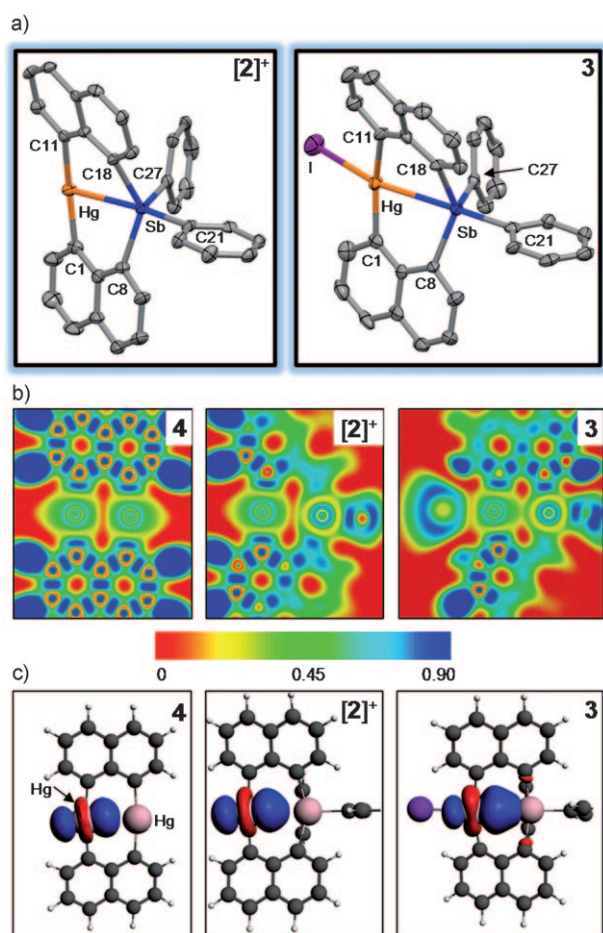


Figure 1. a) Crystal structure of **2**-PF₆ (left) and **3** (right). Thermal ellipsoids are set at 50% probability; hydrogen atoms and the hexafluorophosphate anion of **2**-PF₆ are omitted for clarity. Pertinent metrical parameters can be found in the text and in the Supporting Information. b) ELF maps for [2]⁺, **3**, and **4**. The maps are drawn in the plane containing the two central heavy atoms and one of mercury-bound carbon atoms. c) Mercury-centered Boys orbitals for [2]⁺, **3**, and **4** (at 0.02 isosurface value).

indicates that the antimony atom approaches a distorted trigonal bipyramidal coordination geometry with the mercury atom as one of the axial ligands. This view is confirmed by the sum of the C27-Sb-C8, C27-Sb-C18, and C8-Sb-C18 angles of 344.0°, which approaches the ideal value of 360°. The crystal structure of **3** (Figure 1a), which displays a virtually unchanged Hg–Sb separation of 3.073(1) Å, shows that the iodide anion is coordinated to the mercury center.^[13] As non-fluorinated diarylmercury complexes do not form isolable adducts with any halides,^[12,15] the coordination of the iodide ligand to the mercury atom of **3** constitutes a distinctive and noteworthy feature. The resulting mercury–iodine distance of 2.991(1) Å in **3** is also shorter than that observed in complexes involving highly Lewis acidic fluorinated organomercurials, such as [(C₆F₅)₂HgI][–] (3.118(2) Å).^[16] Owing to the presence of this iodide ligand, the mercury atom has a distorted square planar geometry, as indicated by the C1–Hg–C11 and I–Hg–Sb angles of 163.1(3)° and 162.24(2)°, respectively. The coordination geometry at the antimony center in **3** remains distorted

trigonal bipyramidal, as indicated by the Hg–Sb–C21 angle of 179.2(2)° and a sum of angles in the equatorial plane of 349.3°. The structure of **1** resembles that of **3** with a bromide instead of an iodide coordinated to the mercury center (see the Supporting Information, Figure S1).^[13] Unlike in **3**, however, the bromide ligand of **1** is also involved in an interaction with the antimony atom of a neighboring molecule, leading to the formation of a centrosymmetrical dimeric structure.

The short Hg–Sb separation observed in these dinuclear complexes and also the distorted trigonal bipyramidal geometry displayed by the antimony atom suggests the possibility of a Hg→Sb interaction. To gain more insight into the presence of such an interaction, we carried out DFT calculations on [2]⁺ and **3** using the ADF program. For comparative purposes, analogous calculations were carried out on dimeric naphthalenediyl mercury (**4**), a compound that features a Hg–Hg distance of only 2.8 Å,^[17] and on the mercury–indium complex (C₁₀H₆)₂Hg(InBr·THF)₂ (**5**), the structure of which has been previously reported.^[8] All calculations, which were carried out at the BP86/TZP level of theory using the zero-order regular approximation (ZORA), produced optimized structures that are in excellent agreement with those observed experimentally (see the Supporting Information). The molecular orbitals obtained by these calculations for [2]⁺ and **3** are extensively delocalized on the ligands and do not provide a clear depiction of the antimony–mercury transannular interaction. For this reason, we decided to use the electron localization function (ELF), which can be used to map the electron-pair localization in a molecule.^[18] The ELF values near the mercury–mercury centroid for **4** (Figure 1b) and mercury–indium centroid for **5** (Supporting Information, Figure S2) drop to almost zero, thus indicating the absence of covalent bonding between the two heavy atoms (Figure 1b). In the case of **4**, the ELF analysis is in agreement with the work of Pyykkö who showed that the short mercury–mercury contact present in **4** is nonbonding and repulsive.^[19] In the case of [2]⁺, the region of low ELF values separating the two heavy atoms shows a distinct thinning, thus signaling the onset of covalent bonding. This phenomenon becomes much more acute in **3**, as shown by a continuum of elevated ELF values along the Hg→Sb vector. This feature indicates that the coordination of the iodide to the mercury center increases the donor capability of the latter toward the antimony atom. Further evidence for the electron sharing in the Hg→Sb linkage was derived from a Boys localization analysis (Figure 1c). In all cases, this analysis identifies a lone pair at mercury of d character that is clearly extended along the transannular vector. This lone pair shows essentially no polarization in the case of **4** (Figure 1c) and **5** (Supporting Information, Figure S2). On going from [2]⁺ to **3**, this orbital becomes more polarized toward the antimony atom, thus supporting the crucial role played by the iodide in increasing the donor capability of the mercury atom. Altogether, these computational results show that the Hg→Sb present in **3** involves a polar covalent component that complements the strong mercurate–stibonium electrostatic interaction already present in this compound.^[20]

Although these results suggest the participation of d orbitals in the mercury–antimony interaction present in **3**,

it is also possible that this linkage benefits from a I-Hg-Sb three-center–two-electron (3c,2e) interaction that would involve an iodide lone pair orbital, a mercury 6p orbital, and a Sb-C_{ph} σ* orbital (Figure 2a). In support of this view, we note that the LUMO of [2]⁺ bears a large contribution from the latter two orbitals (Figure 2b).

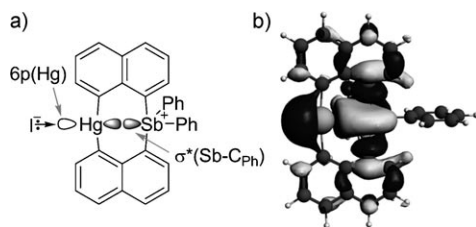


Figure 2. a) I-Hg-Sb 3c,2e interaction in **3**. b) Lowest unoccupied molecular orbital of [2]⁺ (at 0.02 isosurface value) showing the large contribution from the mercury 6p and Sb-C_{ph} σ* orbitals.

In conclusion, we have demonstrated that the mercury center of **3** can act as a Lewis base, a phenomenon that had thus far only been observed for transition metals. In the case of **3**, this phenomenon is the result of a unique iodide push–sibonium pull effect, which polarizes the diffuse closed shell of the mercury atom, thus promoting its engagement in a polar bonding interaction.

Experimental Section

Caution! Mercury, antimony, and thallium compounds are highly toxic and should be handled cautiously. Mercuric bromide and triphenylantimony were purchased from Aldrich. Thallium hexafluorophosphate was purchased from Alfa Aesar. 1,8-Dilithionaphthalene-tmeda^[10] and triphenyldibromoantimony^[21] were prepared according to published procedures. All preparations were carried out under an atmosphere of dry N₂ employing either a glove box or standard Schlenk techniques. Solvents were dried by passing through an alumina column (*n*-pentane and MeCN) or refluxing under N₂ over Na/K (Et₂O, *n*-hexane, and THF). NMR spectra were recorded on a Varian Unity Inova 400 FT NMR spectrometer (¹H: 399.59 MHz, ¹³C: 100.45 MHz, ¹⁹⁹Hg: 71.20 MHz) at ambient temperature. Chemical shifts δ are given in ppm and are referenced to residual ¹H and ¹³C solvent signals and external neat HgMe₂.

1: A solution of Ph₃SbBr₂ (500 mg, 0.976 mmol) in THF (10 mL) was added dropwise to a solution of 1,8-dilithionaphthalene-tmeda (250 mg, 0.976 mmol) in THF (5 mL) at ambient temperature. The mixture was allowed to stir for 10 min and was then transferred into a THF solution (3 mL) of HgBr₂ (352 mg, 0.976 mmol). The resulting clear yellow solution was allowed to stand overnight at room temperature, yielding yellow crystals of complex **1** (213 mg, 54% yield), which were filtered, washed with THF (3 × 5 mL), and dried under vacuum. ¹H NMR (400 MHz; [D₆]DMSO) δ = 8.98 (d, 2H, Naph-CH, ³J_{H-H} = 6.7 Hz), 8.24 (d, 2H, Naph-CH, ³J_{H-H} = 8.0 Hz), 8.08 (d, 2H, Naph-CH, ³J_{H-H} = 8.0 Hz), 7.76 (d, 2H, Naph-CH, ³J_{H-H} = 7.2 Hz), 7.71 (t, 2H, *p*-Ph-CH, ³J_{H-H} = 7.4 Hz), 7.57–7.44 (m, 8H, *m*-Ph-CH and Naph-CH), 7.19 ppm (d, 4H, *o*-Ph-CH, ³J_{H-H} = 7.1 Hz); ¹³C NMR (100 MHz; [D₆]DMSO) δ = 173.9, 145.3, 142.4, 140.6, 137.3, 135.8, 135.6, 134.3, 132.7, 131.7, 131.4, 129.7, 128.1, 126.0 ppm; ¹⁹⁹Hg NMR (71 MHz; [D₆]DMSO) δ = –68.2 (s). Elemental analysis calcd (%) for C₃₂H₂₂BrHgSb: C 47.52, H 2.74; found: C 48.10, H 2.74.

2-PF₆: Solid TlPF₆ (17.5 mg, 0.05 mmol) was added in one portion to a MeCN solution (2 mL) of complex **1** (40.6 mg, 0.05 mmol),

resulting in the immediate precipitation of TlBr, which was removed by filtration through celite. Pentane (10 mL) was added to the filtrate, resulting in the precipitation of **2-PF₆** (29.8 mg, 68% yield) as a white solid. Further recrystallization of the solid from MeCN (3 mL) afforded colorless crystals of **2-PF₆**·MeCN. ¹H NMR (400 MHz; [D₆]DMSO) δ = 8.28 (d, 2H, Naph-CH, ³J_{H-H} = 7.7 Hz), 8.20 (d, 2H, Naph-CH, ³J_{H-H} = 6.7 Hz), 8.09 (d, 2H, Naph-CH, ³J_{H-H} = 8.0 Hz), 7.80–7.77 (m, 4H, *p*-Ph-CH and Naph-CH), 7.58–7.49 (m, 8H, *m*-Ph-CH and Naph-CH), 7.19 ppm (bs, 4H, *o*-Ph-CH); ¹³C NMR (100 MHz; [D₆]DMSO) δ = 171.8, 142.5, 140.4, 138.0, 136.5, 135.0, 133.3, 132.6, 131.9, 130.6, 128.7, 127.0, 125.4 ppm (one of the quaternary carbon nuclei was not detected); ¹⁹⁹Hg NMR (71 MHz; [D₆]DMSO) δ = –271.9 ppm (s). HRMS: *m/z* calcd for C₃₂H₂₂HgSb⁺ 729.0461; found: 729.0463.

3: To a yellow suspension of **1** (20 mg, 0.025 mmol) in THF (2 mL), TlPF₆ (1.2 equiv, 10.4 mg, 0.030 mmol) was added at room temperature, resulting in the formation of a white precipitate of TlBr. 2.0 equiv of solid tetrabutylammonium iodide (18.5 mg, 0.050 mmol) was added to this mixture in one portion. After stirring for 10 min, the precipitate was removed by filtration through celite, and the resulting solution was allowed to stand for 24 h at –20 °C, leading to the formation **3** as yellow crystals (18 mg, 85% yield). ¹H NMR (400 MHz; [D₆]DMSO) δ = 8.84 (d, 2H, Naph-CH, ³J_{H-H} = 6.8 Hz), 8.27 (d, 2H, Naph-CH, ³J_{H-H} = 8.0 Hz), 8.09 (d, 2H, Naph-CH, ³J_{H-H} = 8.0 Hz), 7.78 (d, 2H, Naph-CH, ³J_{H-H} = 7.4 Hz), 7.73 (t, 2H, *p*-Ph-CH, ³J_{H-H} = 7.5 Hz), 7.59–7.46 (m, 8H, *m*-Ph-CH and Naph-CH), 7.20 ppm (d, 4H, *o*-Ph-CH, ³J_{H-H} = 7.6 Hz); ¹³C NMR (100 MHz; [D₆]DMSO) δ = 174.0, 144.4, 142.4, 140.6, 137.3, 135.7, 134.3, 133.1, 132.7, 131.6, 131.4, 129.6, 128.0, 126.0 ppm; ¹⁹⁹Hg NMR (71 MHz; [D₆]DMSO) δ = –71.8 ppm (s). Elemental analysis calcd (%) for C₃₂H₂₂HgISb: C 44.91, H 2.59; found: C 44.97, H 2.52.

DFT structural optimizations were carried out using the ADF program (2008.01).^[22] All calculations were carried out using the BP86 functional^[23] with the all-electron TZP basis sets for all atoms.^[24] These calculations were performed using the zero-order regular approximation (ZORA).^[25] Electron localization function (ELF)^[18] and Boys^[26] localization analyses were carried out in the ADF program. ELF plots and Boys localized orbitals were visualized in the ADF program.

Received: May 17, 2010

Published online: July 26, 2010

Keywords: antimony · hypervalence · Lewis acids · mercury · transition metals

- [1] a) R. L. Deming, A. L. Allred, A. R. Dahl, A. W. Herlinger, M. O. Kestner, *J. Am. Chem. Soc.* **1976**, *98*, 4132–4137; b) P. Hrobárik, M. Kaupp, S. Riedel, *Angew. Chem.* **2008**, *120*, 8759–8761; *Angew. Chem. Int. Ed.* **2008**, *47*, 8631–8633; c) S. Riedel, M. Straka, M. Kaupp, *Chem. Eur. J.* **2005**, *11*, 2743–2755.
- [2] X. Wang, L. Andrews, S. Riedel, M. Kaupp, *Angew. Chem.* **2007**, *119*, 8523–8527; *Angew. Chem. Int. Ed.* **2007**, *46*, 8371–8375.
- [3] a) M. Kaupp, H. G. von Schnering, *Angew. Chem.* **1993**, *105*, 952–954; *Angew. Chem. Int. Ed. Engl.* **1993**, *32*, 861–863; b) M. Kaupp, M. Dolg, H. Stoll, H. G. von Schnering, *Inorg. Chem.* **1994**, *33*, 2122–2131.
- [4] W. B. Jensen, *J. Chem. Educ.* **2008**, *85*, 1182–1183.
- [5] a) H. Braunschweig, K. Gruss, K. Radacki, *Angew. Chem.* **2007**, *119*, 7929–7931; *Angew. Chem. Int. Ed.* **2007**, *46*, 7782–7784; b) H. Braunschweig, K. Radacki, K. Schwab, *Chem. Commun.* **2010**, *46*, 913–915; c) H. Braunschweig, K. Gruss, K. Radacki, *Angew. Chem.* **2009**, *121*, 4303–4305; *Angew. Chem. Int. Ed.* **2009**, *48*, 4239–4241.
- [6] a) S. Bontemps, G. Bouhadir, K. Miqueu, D. Bourissou, *J. Am. Chem. Soc.* **2006**, *128*, 12056–12057; b) M. Sircoglou, S. Bon-

- temps, M. Mercy, N. Saffon, M. Takahashi, G. Bouhadir, L. Maron, D. Bourissou, *Angew. Chem.* **2007**, *119*, 8737–8740; *Angew. Chem. Int. Ed.* **2007**, *46*, 8583–8586; c) M. Sircoglou, M. Mercy, N. Saffon, Y. Coppel, G. Bouhadir, L. Maron, D. Bourissou, *Angew. Chem.* **2009**, *121*, 3506–3509; *Angew. Chem. Int. Ed.* **2009**, *48*, 3454–3457; d) P. Gualco, T.-P. Lin, M. Sircoglou, M. Mercy, S. Ladeira, G. Bouhadir, L. M. Perez, A. Amgoune, L. Maron, F. P. Gabbaï, D. Bourissou, *Angew. Chem.* **2009**, *121*, 10076–10079; *Angew. Chem. Int. Ed.* **2009**, *48*, 9892–9895.
- [7] a) H. Braunschweig, R. D. Dewhurst, A. Schneider, *Chem. Rev.* **2010**, *110*, 3924–3957; b) J. S. Figueroa, J. G. Melnick, G. Parkin, *Inorg. Chem.* **2006**, *45*, 7056–7058; c) K. Pang, S. M. Quan, G. Parkin, *Chem. Commun.* **2006**, 5015–5017; d) A. F. Hill, G. R. Owen, A. J. P. White, D. J. Williams, *Angew. Chem.* **1999**, *111*, 2920–2923; *Angew. Chem. Int. Ed.* **1999**, *38*, 2759–2761; e) A. F. Hill, *Organometallics* **2006**, *25*, 4741–4743; f) V. K. Landry, J. G. Melnick, D. Buccella, K. Pang, J. C. Ulichny, G. Parkin, *Inorg. Chem.* **2006**, *45*, 2588–2597; g) J. Wagler, E. Brendler, *Angew. Chem.* **2010**, *122*, 634–637; *Angew. Chem. Int. Ed.* **2010**, *49*, 624–627.
- [8] F. P. Gabbaï, A. Schier, J. Riede, A. Sladek, H. W. Goerlitzer, *Inorg. Chem.* **1997**, *36*, 5694–5698.
- [9] a) V. Gutmann, H. Hubacek, A. Steininger, *Monatsh. Chem.* **1964**, *95*, 678–686; b) G. A. Olah, W. S. Tolgyesi, S. J. Kuhn, M. E. Moffatt, I. J. Bastien, E. B. Baker, *J. Am. Chem. Soc.* **1963**, *85*, 1328–1334.
- [10] W. Neugebauer, T. Clark, P. v. R. Schleyer, *Chem. Ber.* **1983**, *116*, 3283–3292.
- [11] M. A. Sens, N. K. Wilson, P. D. Ellis, J. D. Odom, *J. Magn. Reson.* **1975**, *19*, 323–336.
- [12] V. B. Shur, I. A. Tikhonova, *Russ. Chem. Bull.* **2003**, *52*, 2539–2554.
- [13] CCDC 771798, CCDC 771799, and CCDC 771800 contain the supplementary crystallographic data for this paper. These data can be obtained free of charge from The Cambridge Crystallographic Data Centre via www.ccdc.cam.ac.uk/data_request/cif.
- [14] B. Cordero, V. Gomez, A. E. Platero-Prats, M. Reyes, J. Echeverria, E. Cremades, F. Barragan, S. Alvarez, *Dalton Trans.* **2008**, 2832–2838.
- [15] a) T. J. Taylor, C. N. Burrell, F. P. Gabbaï, *Organometallics* **2007**, *26*, 5252–5263; b) T. J. Wedge, M. F. Hawthorne, *Coord. Chem. Rev.* **2003**, *240*, 111–128.
- [16] F. Schulz, I. Pantenburg, D. Naumann, *Z. Anorg. Allg. Chem.* **2003**, *629*, 2312–2316.
- [17] H. Schmidbaur, H. J. Oeller, D. L. Wilkinson, B. Huber, G. Mueller, *Chem. Ber.* **1989**, *122*, 31–36.
- [18] A. D. Becke, K. E. Edgecombe, *J. Chem. Phys.* **1990**, *92*, 5397–5403.
- [19] P. Pyykkö, M. Straka, *Phys. Chem. Chem. Phys.* **2000**, *2*, 2489–2493.
- [20] A Morokuma-type energy decomposition analysis carried out with the ADF program on the model complex $\text{IH}_2\text{Hg} \rightarrow \text{SbH}_2\text{Ph}_2$ indicates that the IH_2Hg and SbH_2Ph_2 fragments are held by an electrostatic interaction of $-354.390 \text{ kJ mol}^{-1}$ and an orbital interaction of $-171.351 \text{ kJ mol}^{-1}$. Further details can be found in the Supporting Information.
- [21] M. Kimura, A. Iwata, M. Itoh, K. Yamada, T. Kimura, N. Sugiura, M. Ishida, S. Kato, *Helv. Chim. Acta* **2006**, *89*, 747–783.
- [22] a) ADF2008.01. SCM, Theoretical Chemistry, Vrije Universiteit, Amsterdam, The Netherlands, <http://www.scm.com>; b) C. Fonseca Guerra, J. G. Snijders, G. te Velde, E. J. Baerends, *Theor. Chem. Acc.* **1998**, *99*, 391–403; c) G. te Velde, F. M. Bickelhaupt, E. J. Baerends, C. F. Guerra, S. J. A. van Gisbergen, J. G. Snijders, T. Ziegler, *J. Comput. Chem.* **2001**, *22*, 931–967.
- [23] a) A. D. Becke, *Phys. Rev. A* **1988**, *38*, 3098–3100; b) J. P. Perdew, *Phys. Rev. B* **1986**, *33*, 8822–8824.
- [24] E. van Lenthe, E. J. Baerends, *J. Comput. Chem.* **2003**, *24*, 1142–1156.
- [25] a) E. van Lenthe, E. J. Baerends, J. G. Snijders, *J. Chem. Phys.* **1993**, *99*, 4597–4610; b) E. van Lenthe, E. J. Baerends, J. G. Snijders, *J. Chem. Phys.* **1994**, *101*, 9783–9792; c) E. van Lenthe, R. van Leeuwen, E. J. Baerends, J. G. Snijders, *Int. J. Quantum Chem.* **1996**, *57*, 281–293; d) E. van Lenthe, J. G. Snijders, E. J. Baerends, *J. Chem. Phys.* **1996**, *105*, 6505–6516; e) E. van Lenthe, A. Ehlers, E.-J. Baerends, *J. Chem. Phys.* **1999**, *110*, 8943–8953.
- [26] a) J. M. Foster, S. F. Boys, *Rev. Mod. Phys.* **1960**, *32*, 300–302; b) C. Edmiston, K. Ruedenberg, *Rev. Mod. Phys.* **1963**, *35*, 457–464; c) W. Von Niessen, *J. Chem. Phys.* **1972**, *56*, 4290–4297.